



Biometric analysis hand parameters in young adults for prosthetic hand and ergonomic product applications

Gkionoul Nteli Chatzioglou^{1,2}, Yelda Pınar¹, Figen Govsa¹

¹Department of Anatomy, Digital Imaging and 3D Modeling Laboratory, Faculty of Medicine, Ege University, Izmir, ²Department of Anatomy, Faculty of Medicine, Istanbul Health and Technology University, Istanbul, Turkey

Abstract: This study aimed to evaluate the superficial anatomy, kinesiology, and functions of the hand to reveal its morphometry and apply the findings in various fields such as prosthetic hand and protective hand support product design. We examined 51 young adults (32 females, 19 males) aged between 18–30. Hand photographs were taken, and measurements were conducted using ImageJ software. Pearson correlation analysis was performed to determine the relationship between personal information and the parameters. The results of the measurements showed the average lengths of finger segments: thumb (49.5±5.5 mm), index finger (63.9±4.1 mm), middle finger (70.7±5.2 mm), ring finger (65.5±4.8 mm), and little finger (53.3±4.3 mm). Both females and males, the left index finger was measured longer than the right index finger. The right ring finger was found to be longer than the left in both sexes. Additionally, length differences between fingers in extended and maximally adducted positions were determined: thumb-index finger (56.1±6.2 mm), index-middle finger (10.7±4.1 mm), middle-ring finger (10.8±1.4 mm), and ring-little finger (25.6±2.7 mm). Other findings included the average radial natural angle (56.4°±10.5°), ulnar natural angle (23.4°±7.1°), radial deviation angle (65.2°±8.2°), ulnar deviation angle (51.2°±9.6°), and grasping/gripping angle (49.1°±5.8°). The average angles between fingers in maximum abduction positions were also measured: thumb-index finger (53.4°±6.5°), index-middle finger (17.2°±2.6°), middle-ring finger (14.3°±2.3°), and ring-little finger (32.1°±7.0°). The study examined the variability in the positioning of proximal interphalangeal joints during maximum metacarpophalangeal and proximal interphalangeal flexion, coinciding with maximum distal interphalangeal extension movements. The focal points of our observations were the asymmetrical and symmetrical arches formed by these joints. This study provides valuable hand parameters in young adults, which can be utilized in various applications such as prosthetic design, ergonomic product development, and hand-related research. The results highlight the significance of considering individual factors when assessing hand morphology and function.


Key words: Anatomy, Hand, Biometry, Ergonomics, Fingers

Received December 26, 2023; Accepted January 10, 2024

Introduction

The human hand is a remarkable organ that possesses unique characteristics in terms of its neural, muscular, and skeletal structure, allowing for a wide range of complex finger movements and fine motor control (Fig. 1) [1-4]. It plays a vital role in our daily activities, enabling us to perform tasks such as buttoning a shirt, using a smartphone, or conducting

Corresponding author:

Gkionoul Nteli Chatzioglou 
Department of Anatomy, Faculty of Medicine, Istanbul Health and
Technology University, Istanbul 34500, Turkey
E-mail: gkionoul.chatzioglou@istun.edu.tr

Copyright © 2024. Anatomy & Cell Biology

This is an Open Access article distributed under the terms of the Creative Commons Attribution Non-Commercial License (<http://creativecommons.org/licenses/by-nc/4.0/>) which permits unrestricted non-commercial use, distribution, and reproduction in any medium, provided the original work is properly cited.



Fig. 1. The functional anatomy of the hand; from left to right: adduction of the fingers – maximum abduction of the fingers – radial deviation of the wrist – ulnar deviation of the wrist – maximum flexion of metacarpophalangeal and proximal interphalangeal joints and maximum extension of the distal interphalangeal joint facing the scaphoid bone.

surgical procedures with precision and dexterity [5, 6]. However, due to its frequent use, the hand is also prone to injuries and various forms of physical loss, such as amputations resulting from high-energy traumas, accidents, diseases, or congenital anomalies [7-12].

Hand loss not only affects the functional capabilities of individual fingers but also compromises the overall bilateral hand dexterity [13]. Consequently, individuals with hand loss experience significant challenges and limitations, affecting their quality of life and impeding their participation in social and occupational activities [14]. Prosthetic hands have been developed to address these challenges and enhance the well-being of individuals with hand loss, enabling them to regain their independence and engage in daily activities [15].

However, there are significant issues that need to be addressed in protective hand support products and prosthetic hand design, as they often present challenges and limitations that hinder their usability. High cost, bulky and heavy designs, limited range of motion, skin irritation, and discomfort due to excessive sweating are some of the limitations associated with traditional prosthetic hands [13, 15].

Recently, three-dimensional (3D) printing technology has gained popularity as cost-effective and lightweight alternatives in prosthetic hand development. Utilizing 3D technology allows for the production of customizable and affordable support products and prosthetic hands [15, 16]. An important criterion in prosthetic hand design is anatomical compatibility. Anthropometric measurements of the hand provide critical data for the ergonomic and functional design of protective products and prosthetic hands, ensuring natural appearance and preserved mobility [17, 18]. The lack of personalized design, discomfort during use, pain and pressure sensations during movement, increased weight and size compared to a natural hand, and limited range of motion are common reasons why individuals discontinue prosthetic hand use.

This study aims to address these issues and develop user-

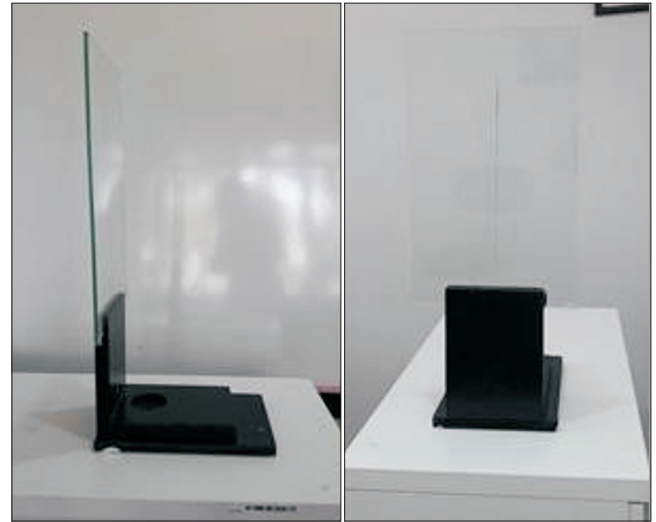


Fig. 2. Material designed for photo shoots and used during photo shoot.

friendly hand support products and prosthetic solutions, it is essential to conduct morphometric measurements that uncover the limitations of existing designs and facilitate improvements in prosthetic functionality and design.

Materials and Methods

This study was ethically approved by the Non-Invasive Clinical Research Ethics Committee of the Faculty of Medicine at Ege University, with decision number 70198063-050.06.04 dated October 3, 2016. The work as photoanthropometric image analysis was carried out in the Digital Imaging and 3D Modeling Laboratory of the Department of Anatomy at Ege University.

Subject

A total of 51 healthy young adults, with an age average of 18–30, were randomly included in the study. Only individuals with no functional impairments or deformities in their

forearms and hands were included. Information was also collected from participants through a survey, which included past upper extremity injuries, surgeries, job positions, instrument/sport engagements, dominant hand, hand used for writing, and demographic information.

A device made of glass and wood was designed for the measurements (Fig. 2). The wooden part included a section for the volunteers to place their elbow, allowing photographs to be taken while maintaining the anatomical position of the forearm-wrist-hand. A vertical line was drawn on the glass part.

Details of photograph

Photographs were taken using a Nikon DX AF-NIKKOR camera (Nikon) along with a tripod. Length and angle measurements were made from the photos taken with various

hand and finger positions in the frontal plane. The photos were evaluated using the Image J 2D computer program, and the data was recorded.

Measurements for the study were made at the same time of day, in the same environment, using the same measuring tools (camera-meter-digital scale) by the same person. In each length measurement, a conversion from pixels to millimeters was made using the formula $0.08618 \times$ measured length in pixel value.

Measurements techniques

The measurements of the volunteers were made based on the following nine parameters in total.

1. Calculation of finger length: the length of each finger from the first proximal fold to the peak of the distal phalanx was measured and recorded (Fig. 3). Length of left (LTL) and right (LTR) thumbs; index fingers length, left (LIL), right (LIR); middle fingers length, left (LML), right (LMR); ring fingers length, left (LRL), right (RR); and little fingers length, left (LLL), right (LLR).

2. Measurement of differences between the lengths of the distal phalanxes (DP) (Fig. 4).

3. Radial natural angle (RDA): this is the angle between the line drawn from the thenar region to the median line while the fingers are in maximum adduction (Fig. 5A, B).

4. Ulnar natural angle (UDA): this is the angle between the line drawn from the hypothenar region to the parallel line towards the median line while the fingers are in maximum adduction (Fig. 6A, B).

5. Radial deviation (radial abduction) angle (RD): this is the angle between the line taken from the thenar region and the parallel line drawn to the median error when the wrist is at maximum radial deviation (Fig. 5C, D).

6. Ulnar deviation (ulnar abduction) angle (UD): this is

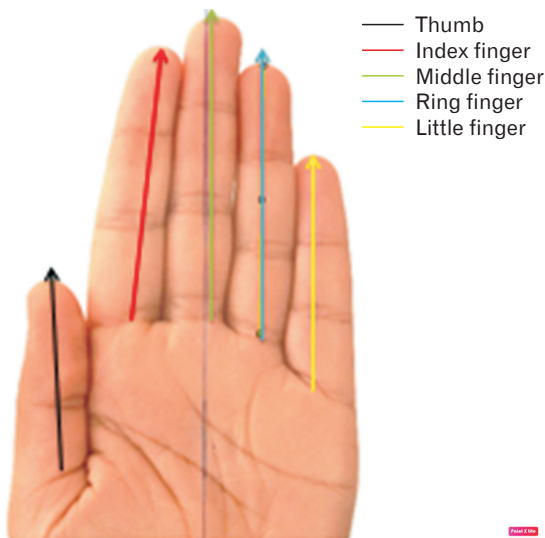


Fig. 3. Schematic view of calculation the lengths of each finger on the hand.

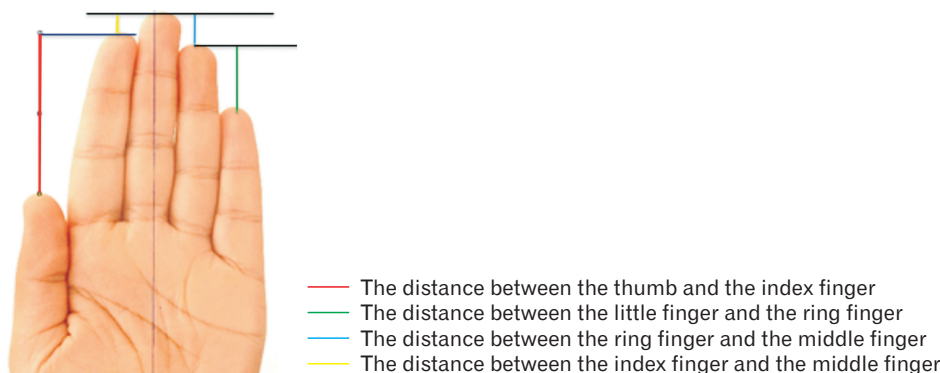


Fig. 4. Schematic view of calculation of the difference in length between the fingers.

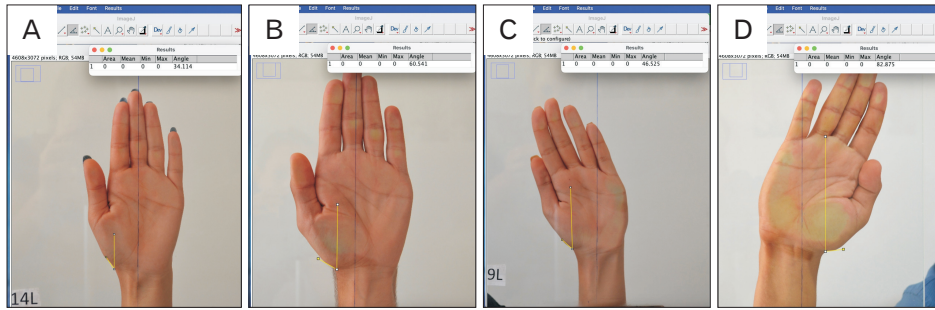


Fig. 5. View of the radial natural angle and radial deviation angles. (A) Minimum radial natural angle. (B) Maximum radial natural angle. (C) Minimum radial deviation angle. (D) Maximum radial deviation angle.

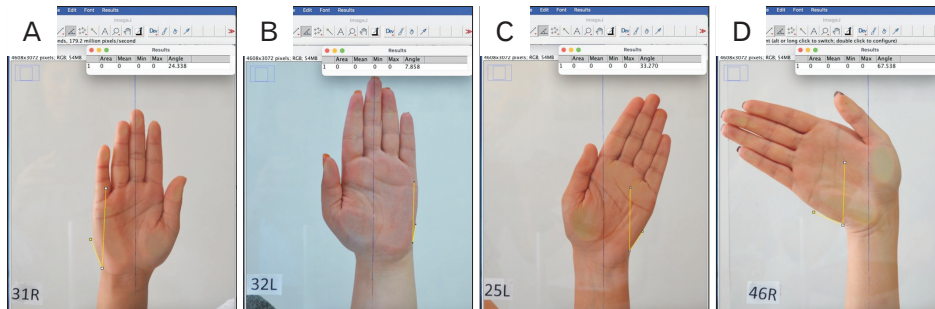


Fig. 6. View of the ulnar natural angle and ulnar deviation angles. (A) Maximum ulnar natural angle. (B) minimum ulnar natural angle. (C) Minimum ulnar deviation angle. (D) Maximum ulnar deviation angle.

the angle between the line taken from the hypothenar region and the parallel line drawn to the median error when the wrist is at maximum ulnar deviation (Fig. 6C, D).

7. Grip/grasp angle (TA): the first line starts from the bend of the proximal phalanx of the fifth finger and ends at the bend of the proximal phalanx of the fourth and third fingers. This line can be practically obtained by joining the points where we measure the lengths of the little finger, ring finger, and middle finger. The second line starts from the bend of the proximal phalanx of the second finger and ends at the proximal phalanx of the third finger (Fig. 7).

8. Angle of fingers in maximum abduction (MAX): The angles where the line passing through the middle of each finger in maximum abduction (median line) intersects are calculated (Fig. 8A–E).

9. Interdigital angle facing the scaphoid bone (SCAP): Except for the thumb, in maximum flexion of the metacarpophalangeal joints, the longitudinal axes of the fingers pass through the scaphoid bone. These are the angles formed between these axes (Fig. 9A–C).

Statistical evaluation of data

Descriptive statistics for study data were evaluated using tables and graphics in the IBM SPSS Statistics 21.0 program (IBM Co.). A normality test was applied to the data transferred to the SPSS program and it was determined that the

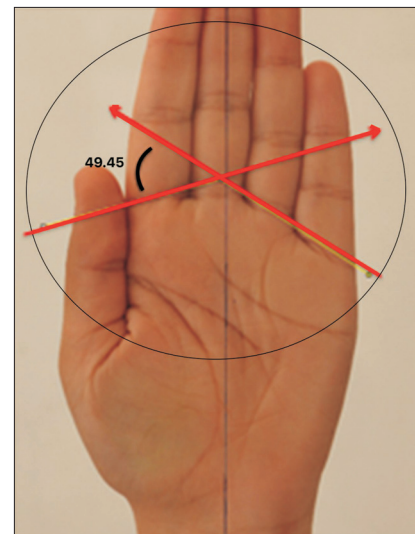


Fig. 7. Calculation method of grip/grasp angle.

data did not distribute normally, and the Mann–Whitney test was applied from non-parametric tests. Right and left measurement values were interpreted using the Wilcoxon signed ranks test. Results were evaluated at a significance level of $P < 0.05$ with 95% reliability. The relationship between all measured values and age, height, and weight values were evaluated with the Pearson correlation analysis.

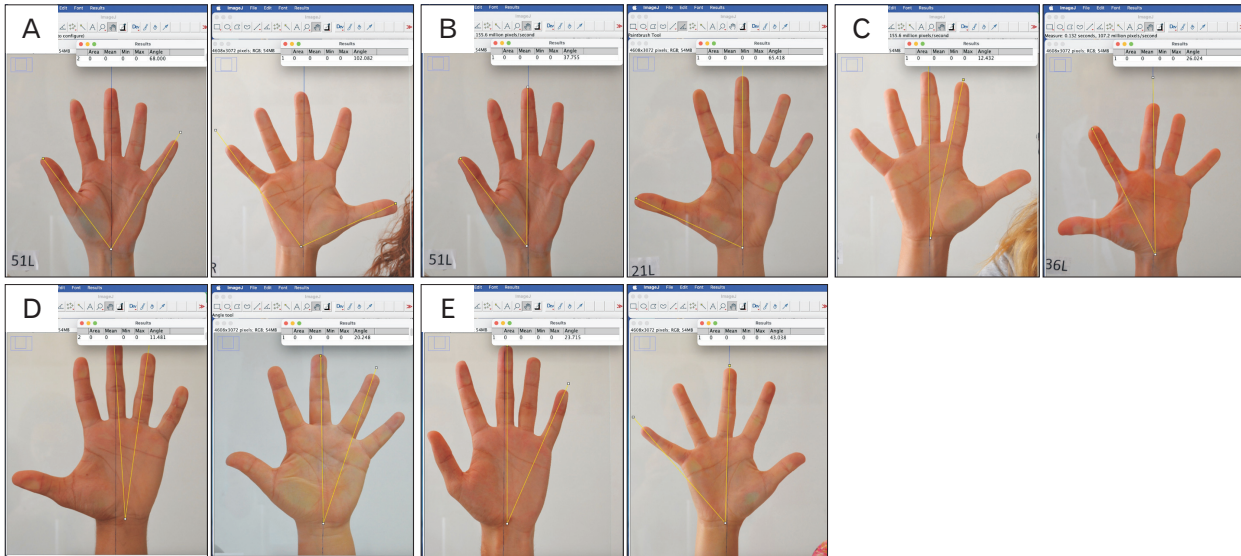


Fig. 8. The angles between the fingers in maximum abduction. (A) Minimum and maximum values of angle occurred between the thumb and the little finger. (B) Minimum and maximum values of angle occurred between the thumb and the third finger. (C) Minimum and maximum values of angle occurred between the second and the third finger. (D) Minimum and maximum values of angle occurred between the third and the fourth finger. (E) Minimum and maximum values of angle occurred between the third and the little finger.

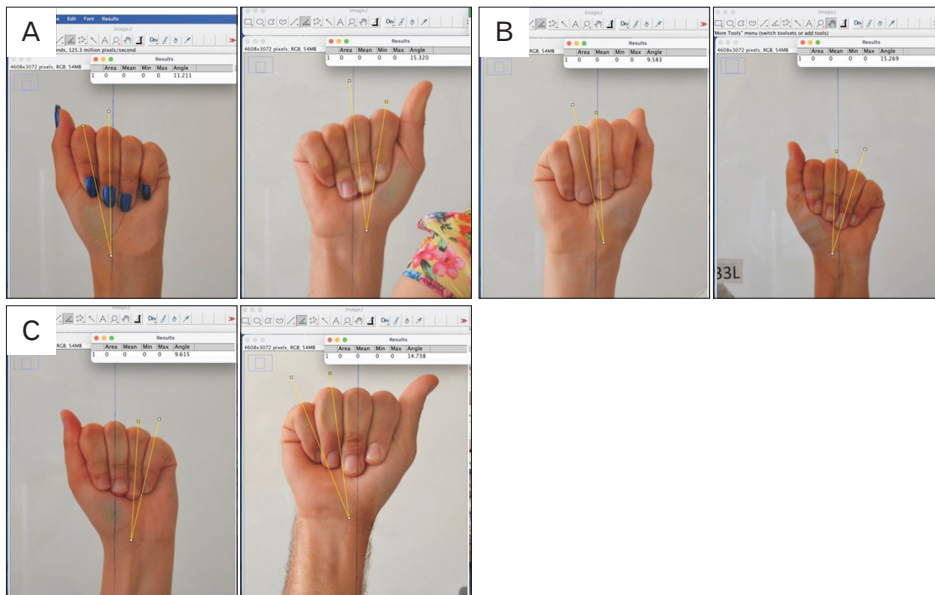


Fig. 9. The minimum and maximum values of the interdigital angles of the fingers brought towards the scaphoid bone and the schematic view of the hand. (A) The angle between the 2nd and the 3rd fingers. (B) The angle between the 3rd and the 4th fingers. (C) The angle between the 4th and the 5th fingers.

Results

The most common ages of the volunteers aged 18–30 were 19 (37.2%) and 18 (13.7%). The heights were measured as 163±6 cm (150–175 cm) in females and 177±5 cm (165–187 cm) in males. Length values were examined in 4 groups. The weight values were measured as 57.6±10.5 kg in females and 63.7±9.9 kg in males. Weight values were examined in 11

subgroups.

Finger length measurements are presented in Table 1. No significant difference was found between the right- and left-hand finger length difference measurements in both sexes. Both females and males, the left index finger was measured longer than the right index finger. The right ring finger was found to be longer than the left in both sexes. In males, the index finger was found to be longer on the right than the left.

Table 1. Measurements values of the distances and angles of fingers by sex

Measurements	Details		Female	Male	P-value	Total	P-value	
Length of finger (mm)	Thumb finger	L	48.8±4.4 (39.3–55.5)	54.3±6.0 (44.0–68.0)	<0.001*	50.9±5.7 (39.3–68)	0.001*	
		R	46.7±4.6 (37.2–53.2)	50.6±5.9 (44.4–62.8)		48.2±5.4 (37.2–62.8)		
	Index finger	L	62.2±3.3 (56.2–69.1)	68.2±2.9 (63.6–73.5)	0.014*	64.5±4.3 (56.2–73.3)	<0.001*	
		R	61.4±3.1 (55.8–68.4)	66.5±2.8 (61.8–71.1)		63.4±3.9 (55.8–71.1)		
	Middle finger	L	67.9±4.8 (52.1–76.3)	75.5±3.3 (69.6–79.9)	0.294	70.7±5.5 (52.1–79.9)	0.573	
		R	67.9±3.4 (62.4–76.5)	75.3±3.7 (69.4–80.5)		70.7±5.1 (62.4–80.5)		
	Ring finger	L	62.5±3.2 (57.9–68.8)	69.8±3.0 (64.8–74.4)	0.005*	65.2±4.7 (57.9–74.4)	0.018*	
		R	63.0±3.3 (56.9–70.1)*	70.6±3.1 (66.1–76.0)*		65.8±4.9 (56.9–76.1)		
	Little finger	L	50.2±3.0 (44.0–54.7)	56.8±2.6 (51.5–61.5)	<0.001*	52.6±4.3 (44.0–61.5)	0.006*	
		R	51.4±2.8 (45.0–56.5)*	58.5±2.6 (54.0–63.0)*		54.1±4.4 (45.0–63.0)		
	Distances between the fingers in the most distal part (DP-mm)	Thumb finger	L	54.0±4.5 (46.1–62.0)	59.9±4.7 (52.7–68.0)	0.131	56.2±5.4 (46.1–68.0)	0.500
			R	52.6±4.7 (40.1–62.3)	62.0±6.2 (53.2–74.2)		56.1±7.0 (40.1–74.2)	
Index finger		L	9.6±1.7 (6.7–14.2)	11.1±2.5 (7.2–16.0)	0.874	10.1±2.2 (6.7–16.0)	0.008*	
		R	10.7±7.3 (5.4–49.0)	12.2±2.7 (8.1–17.8)*		11.2±6.0 (5.4–49.0)		
Middle finger		L	10.8±1.3 (8.5–14.0)	11.6±1.6 (9.3–15.5)*	0.922	11.1±1.5 (8.5–15.5)	0.005*	
		R	10.8±1.3 (8.6–13.4)	10.2±1.4 (7.6–11.9)		10.6±1.4 (7.6–13.4)		
Ring finger		L	25.6±3.4 (20.7–39.1)	27.0±2.3 (23.1–31.7)	0.029*	26.1±3.1 (20.7–39.1)	0.122	
		R	24.6±2.6 (19.1–30.7)	26.0±1.7 (23.3–29.5)		25.1±2.4 (19.1–30.7)		
Angles (°)		Radial natural	L	23.5±7.7 (5.3–49.5)	26.3±3.8 (17.7–31.6)*	0.112	24.5±6.6 (5.3–49.5)	0.003*
			R	21.3±8.6 (9.5–59.3)	24.1±5.4 (16.0–35.3)		22.3±7.6 (9.5–59.3)	
	Ulnar natural	L	23.5±7.7 (5.3–49.5)*	26.3±3.8 (17.7–31.6)*	0.043*	24.5±6.6 (5.3–49.5)	0.044*	
		R	21.3±8.6 (9.5–59.3)	24.1 ±5.4 (16.0–35.3)		22.3±7.6 (9.5–59.3)		
	Radial deviation's	L	63.3±7.3 (46.7–75.3)	66.1±8.7 (53.8–86.6)	0.180	64.4±7.9 (46.7–86.6)	0.190	
		R	64.75±8.57 (36.9–82.3)	68.1±8.3 (52.5–82.7)		66.0±8.5 (36.9–82.7)		
	Ulnar deviation's	L	48.8±10.3 (31.0–73.0)	52.9 ±10.5 (31.3–69.0)	0.112	50.3±10.5 (31.0–73.0)	0.658	
		R	51.4±8.6 (32.7–70.6)	53.3±9.2 (32.8–67.1)		52.1±8.8 (32.8–70.6)		
	Gras/grip	L	50.7±6.1 (38.8–62.4)	47.4±4.6 (39.9–58.3)	0.360	49.5±5.8 (38.8–62.4)	0.390	
		R	50.1±6.3 (40.0–65.1)	46.7±4.0 (37.5–53.4)		48.8±5.7 (37.5–65.1)		
	Values of the fingers with maximum abduction (MAX)	MAX1-3	L	55.1±7.4 (37.1–69.8)	54.9±6.0 (42.6–66.8)	<0.001*	55.0±6.8 (37.1–69.8)	0.140
			R	50.8±6.6 (39.3–65.9)	53.1±5.4 (45.5–64.7)		51.7±6.2 (39.3–65.8)	
MAX2-3		L	18.1±2.8 (13.2–27.1)	16.7±2.0 (13.5–20.1)	0.060	17.5±2.6 (13.2–27.1)	0.610	
		R	16.7±2.4 (11.8–22.6)	17.1±2.9 (12.1–22.6)		16.8±2.6 (11.8–22.6)		
MAX3-4		L	13.9±2.3 (10.4–19.6)	13.4±1.8 (10.2–16.2)	0.010*	13.7±2.1 (10.2–19.6)	0.170	
		R	15.3±2.7 (10.8–20.3)	14.0±2.0 (11.3–17.3)		14.8±2.5 (10.8–20.3)		
MAX3-5		L	31.8±3.2 (26.0–37.2)	30.9±3.3 (23.6–36.1)	0.001*	31.5±3.2 (23.6–37.2)	0.570*	
		R	33.6±3.9 (26.3–42.4)*	31.4±3.3 (24.1–37.9)		32.8±3.8 (24.1–42.4)		

Values are presented as mean±SD (range). L, left; R, right; DP, differences between the lengths of the distal phalanges; MAX, angle of fingers in maximum abduction. The statistical values greater than * $P>0.05$.

In females, a significant difference was found on the left side (62.5%) in the comparison between the little finger and ring finger length difference on the right and left.

Significant differences ($P=0.003$) were found in the comparison of the right and left side RDA in males. A significant statistical difference was found in the comparisons of the UDA on the right- and left-hand in both females and males. The Pearson correlation was used to evaluate the relationship between age, height, and weight results and the 9 pa-

rameters measured. According to the results we obtained from the correlation, as the age increases in females, LTL-LTR, RDAL, MAX2-3L, SCAP3-5R, and SCAP4-5L values increase. In males, however, there is an increase in LIL-LIR, LLL, LMR, and SCAP3-5R.

Correlation related to findings about height indicate that as height increases in females, values of LIL-LIR, LMR, LRL-LLR, LLL-LLR, TDPL-TDPR, SCAP3-5L, SCAP4-5R increase. In males, all finger lengths, both left

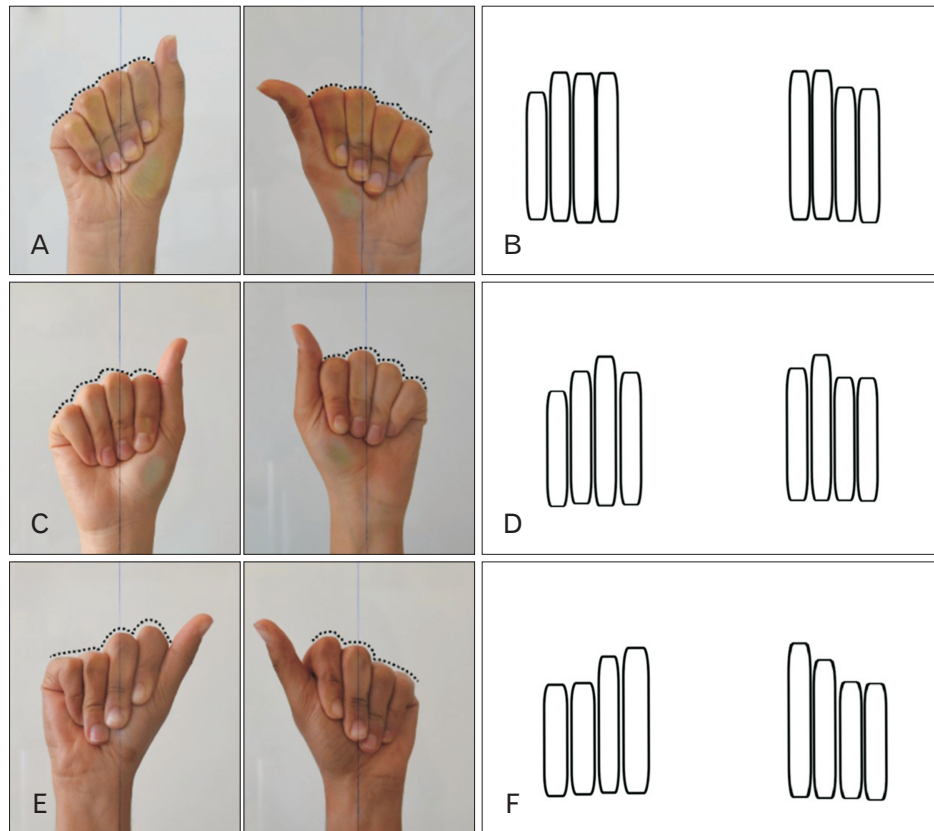


Fig. 10. View of the variable arches of proximal interphalangeal joints during the maximum metacarpophalangeal and proximal interphalangeal flexion with maximum distal interphalangeal extension movements. (A) Asymmetrical arches of proximal interphalangeal joint on the right and left sides. (B) On the right hand the 2nd, 3rd, and 4th arches represent the upper level while the arch of the little finger is found lower, on the left side the 2nd and the 3rd arches are at the same level and at the top while the 4th and the 5th are at the same level but lower (schematic view). (C) Asymmetrical arches of proximal interphalangeal joint on the right and left sides. (D) On the right hand the arch of the 3rd interphalangeal joint is located at the top, while the arch of the little finger is found at the lower, on the left hand although the arch of the 3rd interphalangeal joint is located at the top, the arches of 4th and 5th are lower (schematic view). (E) Symmetrical arches of proximal interphalangeal joint on the right and left sides. (F) Both on the right and the left hands the arch of the 2nd interphalangeal joint is located at the top while the arches of the 3rd and 4th are lower.

and right, as well as TDPL and IDPR, increased with height. When comparing the values of weight results with the 9 parameter values, it was found in females that as weight increases, values of LIL, LIR, LTL-LTR, SCAP2-4R, SCAP2-5L-SCAP2-5R, SCAP3-5R increase. In males, values of LIL, LMR, LRL-LRR, LLL-LLR, TDPL, and MAX3-2L were found to increase with weight.

Dominance of the left hand was found to be higher in males than females. Comparing with parameters, only in males was the value of MAX2-3R found to be associated with the dominant hand. The angle of MAX2-3R is larger in people with dominant left hands ($21.20^{\circ} \pm 2.26^{\circ} > 16.54^{\circ} \pm 2.33^{\circ}$).

This study examines the variability in the positioning of proximal interphalangeal joints during maximum metacarpophalangeal and proximal interphalangeal flexion,

coinciding with maximum distal interphalangeal extension movements (Figs. 9–11). The focal points of our observations were the asymmetrical and symmetrical arches formed by these joints. Three distinct patterns were documented. In the first case, depicted in Fig. 10A, the arches of the proximal interphalangeal joints were asymmetrical on the right and left sides. Specially, Fig. 10B showed that on the right hand, the arches of the 2nd, 3rd, and 4th fingers were situated on a higher level, whereas the arch of the little finger was located lower. In contrast, on the left hand, the arches of the 2nd and 3rd fingers shared the same elevated level, while the 4th and 5th fingers formed an arch on a lower plane. The second pattern, represented in Fig. 10C, maintained the asymmetrical arrangement of the proximal interphalangeal joints on both the right and left sides. However, in this case, as depicted

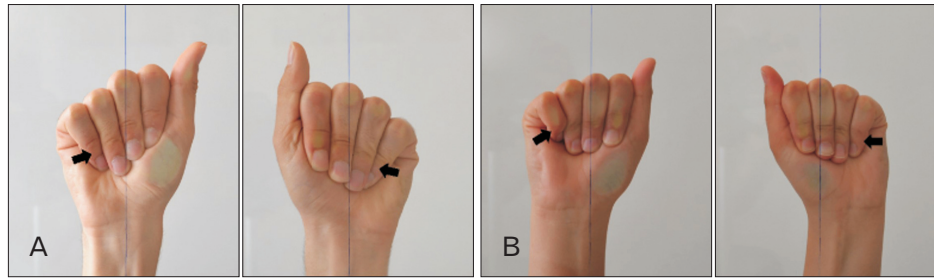


Fig. 11. Variables little finger's position during the metacarpophalangeal and proximal interphalangeal joints flexion and distal interphalangeal joints extension. (A) Abnormal position of the little finger which tends to locate posterior to the 4th finger on both sides. (B) Abnormal flexion of the little finger, during the movement the distal interphalangeal joint is found flexion position on both sides but the on the right side is observes more remarkable.

in Fig. 10D, the 3rd interphalangeal joint of the right hand was positioned at the highest point, and the arch of the little finger was at the lowest. On the left hand, although the 3rd interphalangeal joint's arch was also at the top level, the 4th and 5th fingers' arches were found to be lower. The other pattern (Fig. 10E) illustrated symmetrical arches of the proximal interphalangeal joints on both hands. As depicted in Fig. 10F, on both hands, the 2nd interphalangeal joint's arch was at the highest point, while the arches of the 3rd and 4th fingers were situated lower. This particular configuration resulted in irregular positioning of the fingers during movement.

Our research delves into the peculiarities concerning the positioning of the little finger during the flexion of metacarpophalangeal and proximal interphalangeal joints, as well as during the extension of distal interphalangeal joints. Two significant observations were drawn from this study (Fig. 11). Firstly, in Fig. 11A, an abnormal positioning of the little finger tends to be situated posteriorly to the fourth finger on both hands. The extent of the abnormality varied but was consistently present on both sides. This characteristic positioning during the flexion of the metacarpophalangeal and proximal interphalangeal joints and the extension of the distal interphalangeal joint may offer critical insights into the range of variations in manual dexterity. Secondly, Fig. 11B brought to attention another irregularity. An abnormal flexion of the little finger were identified during movement. Particularly, the distal interphalangeal joint assumed a flexed position on both sides. However, the deviation was markedly pronounced on the right hand. The impact and implications of these peculiarities on fine motor skills, grip strength, and overall hand function require further investigation.

Discussion

Preserving the anatomical integrity and function of the individual's upper limbs essential in the use of prosthetics and protective hand support products [19-21]. However, 35%–45% of prosthetic hand users often abandon the use of products due to the design causing anatomical incompatibility and insufficient comfort. Anatomical incompatibility of the products, constant sensations of pressure, weight, and pain cause the patient to abandon the prosthesis [20, 22]. Factors affecting anatomical compatibility include personal characteristics such as sex, age, weight, and height, the health of the amputated stump area, features of the surgical amputation technique (bone length, new attachment points of muscles, muscle strength, and fat tissue distribution), and the formations that cover and attach the prosthesis from the outside (socket design and direct skeletal attachment) and prosthetic components (control of prosthetic joint movements, activity level) [23, 24].

Although there are many hands prosthetic and support products design that can be made using user-friendly technology and materials, to meet the needs and expectations of amputees, it is necessary to first examine the anatomical and physical features of the hand [8, 12]. The individual not feeling comfortable with the prosthesis, the presence of pain and pressure in the socket in the movable/immobile state, the fact that the prosthesis is heavier and larger than a normal hand, it can make few movements and is slow, the individual quits the use of the prosthesis after a while on the grounds that it is not ergonomic [25-27]. In addition to their current prosthetics being heavy, the fact that only one or two movements can be made reduces the patient's movement limitations and therefore they refuse to use the hand prosthetics they pur-

chased [16, 28]. However, patients want a prosthetic structure that can not only hold a glass with a lighter hand prosthesis, but also perform different hand movements that will perform many activities in daily life such as using a mobile phone, opening a door with a key, spoon holding, capable of lifting a bag, and capable of grasping objects of different hardness without damaging them. In addition, it is desired that hand products should be able to perform skills such as carrying objects, folding clothes, chopping vegetables, which are performed together with both hands as well as movements performed with one hand [29, 30].

Average values of thumb, index finger, middle finger, ring finger, and little finger lengths that we determined as anthropometric measurement were found in many studies being different, and regional characteristics (Table 2) [31, 32]. Anthropometric measurements ensure that the prosthetic hand/hand support products are individualized and appropriate by considering the amputee individual's body mea-

surements and proportions [33-35].

This comprehensive study offers critical insights into the unique variability of hand measurements and joint positioning across a diverse demographic of young adults (Table 2) [27, 36-38]. In exploring the strong correlation between age, height, and weight with nine distinct parameters related to finger lengths, interphalangeal joint positionings, and natural angles, we have underscored the nuanced ways in which these demographic factors influence the biomechanics of the hand. A prominent findings from our results is the variation in finger length across both males and females, with the right ring finger being longer than the left. Interestingly, the difference in finger length between the right and left hands showed no significant difference across sex. However, males tended to have a longer index finger on their right hand compared to their left. In contrast, the females presented a significant difference in the length comparison between the little finger and ring finger on the right and left side, with the left side (62.5%) showing a more substantial discrepancy. For instance, with increasing age in females, we observed increments in LTL-LTR, RDAL, MAX2-3L, SCAP3-5R, and SCAP4-5L values. Similarly, males also demonstrated a correlation with increase in LIL-LIR, LLL, LMR, and SCAP3-5R values. This correlation continued with respect to height, with certain hand parameters increasing as height did. In particular, for females, LIL-LIR, LMR, LRL-LLR, LLL-LLR, TDPL-TDPR, SCAP3-5L, SCAP45-SCAP4-5R values increased with height, and similarly, in males, all finger lengths, both left and right, as well as TDPL and IDPR, increased with height. This implies that height could play a vital role in dictating finger lengths and joint positioning.

When looking at the relationship between height and finger lengths, it was seen that as height increases, finger lengths also increase in both females and males. A difference was found at the 0.05 significance level in the comparison of right- and left-hand lengths of fingers. It was observed that the left index finger length was longer than the right finger in both females and males. In both sexes, it was observed that the LRR was longer than the left. When we examined the distance length difference between fingers, it was found that the TDPL-TDPR and the RDPL-RDPR was almost twice. Thanks to the placement of the thenar muscles that form the bulge on the thenar side of the hand and the localization of the thumb (Fig. 5), the RDA was found to be larger than the UDA in both hands (Fig. 6). In the angle comparison analyses, no significant statistical difference was found

Table 2. Comparison of the morphometric results of finger lengths with the findings in the literature

	Finger length			
	Female		Male	
	Right	Left	Right	Left
Thumb (mm)				
Taner et al. [36]	-	-	57.55±9.36	57.53±8.63
Onat et al. [37]	60.13±4.31	59.54±3.70	67.06±4.51	66.82±4.46
Our study	46.72±4.58	48.81±4.38	50.60±5.91	54.34±6.01
Index finger (mm)				
Lippa [27]	67.54±4.20	68.39±4.24	73.04±4.63	74.24±4.53
Ertuğrul and Otağ [38]	72.32±5.36	72.18±5.18	73.38±4.26	73.56±4.48
Taner et al. [36]	-	-	65.28±7.49	65.64±7.71
Onat et al. [37]	67.03±4.06	67.24±4.13	72.89±4.57	73.63±4.72
Our study	61.43±3.14	62.21±3.32	66.55±2.80	68.22±2.90
Middle finger (mm)				
Taner et al. [36]	-	-	69.98±8.43	71.23±8.38
Onat et al. [37]	76.81±4.19	73.73±4.52	80.47±4.73	80.87±4.86
Our study	67.89±3.42	67.88±4.37	75.34±3.74	75.55±3.33
Ring finger (mm)				
Lippa [27]	70.69±4.29	70.88±4.27	77.46±4.71	77.59±4.72
Ertuğrul and Otağ [38]	74.46±5.53	73.88±5.59	76.75±4.81	75.58±4.48
Taner et al. [36]	-	-	64.82±7.85	64.92±7.56
Onat et al. [37]	68.50±4.32	67.81±4.49	75.76±4.63	74.99±4.65
Our study	63.03±3.33	62.52±3.24	70.57±3.12	69.77±3.03
Little finger (mm)				
Taner et al. [36]	-	-	53.49±7.77	53.55±6.59
Onat et al. [37]	56.08±4.21	54.65±4.30	62.02±4.28	61.04±4.21
Our study	51.44±2.81	50.17±2.96	58.71±2.17	56.82±2.60

in both females and males ($P>0.05$).

In this study, in addition to the evaluation of length and angle measurements related to hands and fingers, the study also focused on the differences and asymmetry of the arc structure of the hand, which was not examined in another research. Significant findings were obtained in the biometrics of the hand. Interestingly, hand dominance showed a marked effect on the interphalangeal joint positions. We observed a higher dominance of the left hand in males than females. In males, the value of MAX2-3R was found to be associated with the dominant hand, with a larger angle of MAX2-3R observed in individuals with left-hand dominance. Finally, our observations on the variability in the positioning of proximal interphalangeal joints during maximum metacarpophalangeal and proximal interphalangeal flexion (Figs. 6, 9) along with maximum distal interphalangeal extension movements (Figs. 5, 8) shed light on three distinct patterns of asymmetrical (Fig. 10A–D) and symmetrical arches (Fig. 10E, F) formed by these joints. These variations could potentially influence the dexterity and functional capability of the hand.

Firstly, the observed variability in the positioning of proximal interphalangeal joints during various movements might reflect the natural morphological diversity among individuals. This diversity could arise from differences in age, sex, occupation, and habitual use of the hands, among other factors. Understanding this variability is critical, as it could influence everything from how we assess and diagnose joint abnormalities to how we design tools, equipment, and devices that are ergonomically suited for different hands.

Secondly, the observed asymmetry in joint positioning between the left and right hands could have implications for hand dominance and the differential development of motor skills between hands. These differences could also be related to handedness, where one hand is more skilled and coordinated for tasks requiring fine motor control.

Thirdly, the abnormal positioning and flexion of the little finger, especially during complex movements, could be indicative of potential underlying musculoskeletal disorders or conditions. Conditions such as arthritis, joint hypermobility, or even neurological conditions could potentially lead to such observable variations in joint behavior.

However, it is essential to note that while these interpretations provide a broad overview of the potential significance of these findings, additional research is needed to more definitively understand the implications and causes of these

observed variations. A more thorough investigation might include a larger sample size, more diverse participant characteristics, or longitudinal studies tracking changes over time.

The use of anatomical measurements will strengthen our knowledge/engineering technologies infrastructure that enhances the ability of scientists to produce knowledge, consciously use technology, and convert technological developments into health, economic, and social benefits. Scientists will be involved in the study and the findings of the anatomical study will be shared. The data obtained in this study, knowledge accumulation, comparison, and archiving are extremely important as they aim to prepare the groundwork for our future studies.

ORCID

Gkionoul Nteli Chatzioglou:

<https://orcid.org/0000-0003-3728-6930>

Yelda Pınar: <https://orcid.org/0000-0001-6026-3564>

Figen Govsa: <https://orcid.org/0000-0001-9635-6308>

Author Contributions

Conceptualization: GNC. Data acquisition: GNC. Data analysis or interpretation: FG, YP. Drafting of the manuscript: GNC, FG, YP. Critical revision of the manuscript: GNC, FG. Approval of the final version of the manuscript: all authors.

Conflicts of Interest

No potential conflict of interest relevant to this article was reported.

Funding

None.

References

1. Cardoso R, Szabo RM. Wrist anatomy and surgical approaches. *Hand Clin* 2010;26:1-19.
2. Coelho LA, Gonzalez CLR. Growing into your hand: the developmental trajectory of the body model. *Exp Brain Res* 2022; 240:135-45.
3. Leversedge FJ. Anatomy and pathomechanics of the thumb. *Hand Clin* 2008;24:219-29.
4. van Nierop OA, van der Helm A, Overbeeke KJ, Djajadiningrat

- TJ. A natural human hand model. *Vis Comput* 2008;24:31-44.
5. Inouye JM, Valero-Cuevas FJ. Anthropomorphic tendon-driven robotic hands can exceed human grasping capabilities following optimization. *Int J Robotics Res* 2014;33:694-705.
 6. Chatzioglou G, Pinar Y. The biometric parameters of the hand surface at young adults. Paper presented at: National Anatomy Congress; 2017 Sep 25-27; Abant, Turkey.
 7. Completo A, Nascimento A, Neto F. Total arthroplasty of basal thumb joint with Elektra prosthesis: an *in vitro* analysis. *J Hand Surg Eur Vol* 2016;41:930-8.
 8. Damert HG, Kober M, Mehling I. Custom-made wrist prosthesis (uni-2™) in a patient with giant cell tumor of the distal radius: 10-year follow-up. *Arch Orthop Trauma Surg* 2020;140:2109-14.
 9. Jones NF, Graham DJ. Radical resection of a recurrent giant cell tumor of the distal ulna and immediate reconstruction with a distal radio-ulnar joint implant arthroplasty. *Hand (NY)* 2020;15:727-31.
 10. Lalchandani GR, Halvorson RT, Zhang AL, Lattanza LL, Immerman I. Patient outcomes and costs after isolated flexor tendon repairs of the hand. *J Hand Ther* 2022;35:590-6.
 11. Stival F, Michieletto S, Cognolato M, Pagello E, Müller H, Atzori M. A quantitative taxonomy of human hand grasps. *J Neuroeng Rehabil* 2019;16:28.
 12. Wanamaker AB, Whelan LR, Farley J, Chaudhari AM. Biomechanical analysis of users of multi-articulating externally powered prostheses with and without their device. *Prosthet Orthot Int* 2019;43:618-28.
 13. Karaçizmeli C, Çakır G, Tükel D. Robotic hand project. Paper presented at: 2014 22nd Signal Processing and Communications Applications Conference (SIU); 2014 Apr 23-25; Trabzon, Turkey.
 14. Werner D, Alawi SA. Four extremity amputation and bionic prosthesis supply after disseminated intravascular coagulation: a follow-up on functionality and quality of life after bionic prosthesis supply. *World J Plast Surg* 2019;8:146-62.
 15. Theyskens NC, Vandesande W. Dislocation in single-mobility versus dual-mobility trapezometacarpal joint prostheses. *Hand (NY)* 2022 Oct 8 [Epub]. <https://doi.org/10.1177/15589447221124257>
 16. Roche AD, Bailey ZK, Gonzalez M, Vu PP, Chestek CA, Gates DH, Kemp SWP, Cederna PS, Ortiz-Catalan M, Aszmann OC. Upper limb prostheses: bridging the sensory gap. *J Hand Surg Eur Vol* 2023;48:182-90.
 17. Demers LAA, Gosselin C. Kinematic design of a planar and spherical mechanism for the abduction of the fingers of an anthropomorphic robotic hand. Paper presented at: 2011 IEEE International Conference on Robotics and Automation; 2011 May 9-13; Shanghai, China. p. 5350-6.
 18. Matheson AB, Sinclair DC, Skene WG. The range and power of ulnar and radial deviation of the fingers. *J Anat* 1970;107:439-58.
 19. Aguilar-Pereyra JF, Castillo-Castaneda E. Design of a reconfigurable robotic system for flexoextension fitted to hand fingers size. *Appl Bionics Biomech* 2016;2016:1712831.
 20. Amundsen A, Rizzo M, Berger RA, Houdek MT, Frihagen F, Moran SL. Twenty-year experience with primary distal radio-ulnar joint arthroplasty from a single institution. *J Hand Surg Am* 2023;48:53-67.
 21. Spilman HW, Pinkston D. Relation of test positions to radial and ulnar deviation. *Phys Ther* 1969;49:837-44.
 22. Lee J, Kunii TL. Model-based analysis of hand posture. *IEEE Comp Gr Appl* 1995;15:77-86.
 23. Billard A, Kragic D. Trends and challenges in robot manipulation. *Science* 2019;364:eaat8414.
 24. Lin J, Wu Y, Huang TS. Modeling the constraints of human hand motion. Paper presented at: Proceedings Workshop on Human Motion; 2000 Dec 7-8; Austin, TX, USA. p. 121-6.
 25. Dutagaci H, Sankur B, Yörük E. Comparative analysis of global hand appearance-based person recognition. *J Electron Imaging* 2008;17:011018.
 26. Eksioğlu M. Relative optimum grip span as a function of hand anthropometry. *Int J Ind Ergon* 2004;34:1-12.
 27. Lippa RA. Are 2D: 4D finger-length ratios related to sexual orientation? Yes for men, no for women. *J Pers Soc Psychol* 2003; 85:179-88.
 28. Metcalf CD, Notley SV, Chappell PH, Burridge JH, Yule VT. Validation and application of a computational model for wrist and hand movements using surface markers. *IEEE Trans Biomed Eng* 2008;55:1199-210.
 29. Baronio G, Harran S, Signoroni A. A critical analysis of a hand orthosis reverse engineering and 3D printing process. *Appl Bionics Biomech* 2016;2016:8347478.
 30. Hu RX, Jia W, Zhang D, Gui J, Song LT. Hand shape recognition based on coherent distance shape contexts. *Pattern Recognit* 2012;45:3348-59.
 31. Li M, Zhuo Y, He B, Liang Z, Xu G, Xie J, Zhang S. A 3D-printed soft hand exoskeleton with finger abduction assistance. Paper presented at: 2019 16th International Conference on Ubiquitous Robots (UR); 2019 Jun 24-27; Jeju, Korea. p. 319-22.
 32. Savič T, Pavešić N. Personal recognition based on an image of the palmar surface of the hand. *Pattern Recognit* 2007;40:3152-63.
 33. Park G, Kim S. Hand biometric recognition based on fused hand geometry and vascular patterns. *Sensors (Basel)* 2013;13: 2895-910.
 34. Pillai JK, Patel VM, Chellappa R, Ratha NK. Secure and robust iris recognition using random projections and sparse representations. *IEEE Trans Pattern Anal Mach Intell* 2011;33:1877-93.
 35. Sandow MJ, McMahon M. Active mobilisation following single cross grasp four-strand flexor tenorrhaphy (Adelaide repair). *J Hand Surg Eur Vol* 2011;36:467-75.
 36. Taner HA, Gözil R, İşeri E, Buru E, Bahçeliöğlu M. [A comparison of obsessive compulsive disorder, pervasive developmental disorder, and control groups in terms of 2D:4D ratio and finger lengths]. *GMJ* 2016;27:40-4. Turkish.
 37. Onat P, Kan S, Nakkaş EÇ, Eryılmaz T, Kadayıfçı EC. El boyutlarından boy tahmininde sosyoekonomik yapının etkisi. XV Student Symposium Working Group Presentations; 2013.
 38. Ertuğrul B, Otağ İ. [Relationship between sexually dimorphic body morphology and second-to-fourth digit ratio]. *İnsanbil Derg* 2012;1:94-107. Turkish.